Marine Pollution Bulletin 217 (2025) 118061

Contents lists available at ScienceDirect

Marine Pollution Bulletin

journal homepage: www.elsevier.com/locate/marpolbul

Model-based insights into pathways and fate of oil spills in the Mediterranean Sea

Svitlana Liubartseva [a,*], Giovanni Coppini [a], Pierre Daniel [b], Donata Melaku Canu [c], Megi Hoxhaj [d]

[a] CMCC Foundation – Euro-Mediterranean Center on Climate Change – Global Coastal Ocean Division, Bologna, Italy
[b] Météo-France – Département Prévision Marine et Océanographique, Toulouse, France
[c] National Institute of Oceanography and Applied Geophysics – OGS, Trieste, Italy
[d] CMCC Foundation – Euro-Mediterranean Center on Climate Change – Global Coastal Ocean Division, Lecce, Italy

ARTICLE INFO

Keywords:
MEDSLIK-II oil spill model
Copernicus Marine Service
HAVEN oil spill
Monte Carlo statistics
Hazard mapping
Contingency planning

ABSTRACT

To better understand the potential consequences of future oil spill accidents in the Mediterranean Sea, extensive Monte Carlo simulations were performed using the Lagrangian oil spill model MEDSLIK-II. Stratified sampling was based on the hypothetical distribution of oil spill sources linked to the latest observational inventory of oil slicks. The transport of virtual oil spills was forced by currents and winds provided by the Copernicus Marine Service and ECMWF from 2018 to 2021. The processing of over two million virtual spill statistics provided practical information for contingency, offshore oil production perspectives, and ecosystem protection. Oil pollution hazard indices, expressed in probabilistic terms, were mapped on the sea surface and coastlines. Arrival times and the percentage of beached oil were defined, computed, and represented through their probability distributions. The Aegean Sea coastline was found to be the most impacted area, with high coastal hazard indices, short arrival times with a median value of approximately 3.1 days, and significant beached oil fractions of around 30 %. In contrast, the Ionian Sea, Central Mediterranean, and Levantine Sea showed relatively low hazard indices, longer arrival times, and smaller beached oil percentages, due to the high dissipative properties of these subbasins. These hazard indices could be incorporated into a multi-hazard assessment and aid in risk assessments. The arrival time and beached oil fraction statistics could be used to plan the development of offshore oil production fields and to minimize the risks of maritime oil transfer activities.

1. Introduction

The negative effects of oil spills on marine life, including plankton, fish, marine birds, turtles, and mammals, can be devastating and long-lasting. Spilled oil emits toxic volatile chemicals into the atmosphere, fouls shorelines, and destroys commercial fisheries, aquaculture, and shellfish beds (ITOPF, 2014a, 2014b; Barron et al., 2020). Oil-associated heavy metals can enter the food chain, accumulating in tissues and poisoning biota (Sharma et al., 2024). Moreover, oil spillages can also seriously affect human health (e.g., Landrigan et al., 2020).

The petroleum hydrocarbon contamination is compounded by the recent inventory by Dong et al. (2022), who revealed that the present-day anthropogenic contribution to marine oil pollution may have been substantially underestimated. The Mediterranean's chronic oil pollution, recently reported by SkyTruth Cerulean,[1] also presents a negative picture.

Furthermore, the recent extreme oil spill in the Black Sea (over 3000 tons of heavy fuel oil near the Kerch Strait, December 2024) revealed a deficiency in oil drift predictions and a general unpreparedness of the competent authorities.

In response to the current understanding of the harmful effects of pollution caused by petroleum hydrocarbons, the NECCTON project has incorporated oil spill simulations into its integrated model-based approach, which combines pelagic, benthic, and nekton biogeochemical cycles with pollutants as environmental stressors. The project transcends disciplinary boundaries by exploring new data streams.

The NECCTON-2023 stakeholder survey showed that ~34 % of respondents from 84 representatives from 45 countries declared their

* Corresponding author.
E-mail address: svitlana.liubartseva@cmcc.it (S. Liubartseva).

[1] https://skytruth.org/wp-content/uploads/2024/04/SkyTruth_Mediterranean_Analysis_2024.pdf (Accessed online: January 2025).

https://doi.org/10.1016/j.marpolbul.2025.118061
Received 20 March 2025; Received in revised form 22 April 2025; Accepted 26 April 2025
Available online 10 May 2025

interest in oil pollution-related products. Consequently, the project aims to provide two oil pollution hazard indices: at the sea surface and on the coastline. The Monte Carlo technique was used to compute the oil pollution hazard indices for the entire Mediterranean basin for the first time. This is in line with a Digital Twin Ocean[2] concept, which necessitates the digitalization of our knowledge of the ocean.

Monte Carlo simulations rely on repeated random sampling controlled by predefined rules and subsequent statistical analyses. The approach is commonly used in oil spill modeling to investigate uncertain scenarios and effectively conduct stochastic process simulations. This technique has been applied to a wide variety of management tasks. The methodology postulates that oil spill scenarios and meteo-oceanographic conditions in the past were, in a broad statistical sense, similar to those that could occur during future spillage accidents (Price et al., 2003). By randomly sampling a large number of individual trajectories, reliable statistical estimations can be obtained that allow a robust forecast of future pathways and the fate of oil spills (French McCay, 2009; French McCay et al., 2017).

These assessments are designed to meet assistance needs, including strategic decisions regarding response equipment types (oil booms, skimmers, storage containers, chemical dispersants, and absorbents), amounts, locations, and deployment timing. The analysis helps to guide civil protection and clean-up. Identifying environmental and economic resources that could be impacted by oil pollution can aid in managing the local economy and planning to preserve biodiversity.

Many numerical models have been run stochastically to predict the pathways of possible oil spills and analyze associated risks. Most are related to single-point sources, although the distributed sources have also been modeled. For the Mediterranean Sea, the first attempt was by Pizzigalli et al. (2007), who focused on the dispersal pathways of the idealized particles sampled uniformly over the entire basin. Olita et al. (2012) investigated the oil spill sources along the tanker shipping routes in the Strait of Bonifacio for the shoreline risk assessment in the coastal archipelago. Quattrocchi et al. (2021), who implemented a dedicated web-based application, used a similar approach focusing on two important harbors in Sardinia. Virtual oil spills have been sampled in the Port of Taranto (southern Italy), an essential strategic hub in the European logistic chain (Liubartseva et al., 2021).

In response to growing gas and oil exploration and production in the Israeli Exclusive Economic Zone, stochastic simulations of possible oil spills were initiated from oil platforms, pipelines, single-point buoy moorings, and shipping routes (Goldman et al., 2015). Hazards potentially impacting the Sicily coasts regarding offshore oil spills were assessed by Melaku Canu et al. (2015). The authors showed how impacts can be substantially reduced by promptly implementing mitigation strategies. Similarly, oil pollution hazard indices and occurrence probability indices were computed for the oil production platforms in the Mediterranean (Olita et al., 2019). The potential impact of oil spills around Cyprus was modeled by Souza et al. (2023).

In planning our simulations, we primarily followed the Oil Spill Risk Analysis (OSRA) model, which has been run by the Bureau of Ocean Energy Management (BOEM) since the 1970s (Smith et al., 1982; Price et al., 2003; Li et al., 2021). The objective of this tool is to calculate the probability of potential oil spills impacting environmental and economic resources based on various spill scenarios before leasing. The occurrence of oil spills has been fundamentally postulated as a matter of probability, which is affected by multiple uncertainties. External forcing, including ocean currents, waves, and wind, have been identified as the key players.

With enormous spatial coverage of up to thousands of kilometers and a timescale of several decades, OSRA requires substantial computational resources and uses fast and efficient algorithms. The latest developments additionally provide the return period of a catastrophic oil spill on the US outer continental shelf and the probability of oil spill contact with vulnerable resources (Ji et al., 2021).

Due to the lack of reliable statistics in the Mediterranean (Polinov et al., 2021), we were unable to evaluate the return period for large-scale hydrocarbon spills by applying extreme value theory as was done with OSRA (Ji et al., 2021). However, we sampled virtual oil spills using the oil spill model MEDSLIK-II, in contrast to OSRA, which uses simplified particle tracking. By mobilizing comprehensive computational resources, we fill the gap in oil pollution hazard mapping in the Mediterranean basin. For the first time, virtual spills were sampled from long-term observational statistics (Dong et al., 2022). In addition to the hazard indices, we computed maps of the arrival times and beached oil fractions, which could have a wide range of practical applications.

The paper is structured as follows: Section 2 describes the MEDSLIK-II oil spill model and the operational meteorological and oceanographic datasets used. Section 3 introduces a virtual spill scenario based on the historical *HAVEN* oil spill accident, presents the Monte Carlo algorithm, and details the hazard calculations. Section 4 reports the results obtained. This is followed by a discussion of the method's strengths, uncertainties, and limitations in Section 5. Finally, Section 6 provides a summary of the key findings and their possible applications.

2. Models and data

2.1. The oil spill model: MEDSLIK-II

The MEDSLIK-II[3] Lagrangian oil spill model (De Dominicis et al., 2013a) is a free-access community model that has been successfully used for over 12 years to simulate the transport and fate of oil spills. A full list of the published MEDSLIK-II applications can be found on the corresponding website.

In the model framework, the oil slick is divided into constituent particles. The problem is represented by stochastic differential equations, which take into account the advection of particles by currents, wind (the so-called wind drift), and waves (De Dominicis et al., 2013a). External oceanographic and atmospheric models or observations provide data on these drivers. Turbulent diffusion is represented as a three-dimensional random walk process. Three states of a particle are considered: floating on the sea surface, dispersed in the water column, and attached to the coastline or beached. For a given particle, the state transition is governed by oil transformations in the environment.

These transformations are computed through bulk formulae, which formalize the changes in thick and thin oil volumes due to three main processes known collectively as weathering: viscous-gravity spreading, evaporation, and natural dispersion. The formation of water-in-oil emulsion is also considered. The model simulates the adsorption of particles into the coastal environment, taking into account the likelihood of being washed back into the water.

With MEDSLIK-II, we computed the geographical coordinates of particles at each time step. By binning the particles of each state, we obtained oil concentrations at the sea surface, in the water column, and along coastlines.

The components of the oil mass balance were calculated and represented as functions of time. The model enables oil types to be selected from the Regional Marine Pollution Emergency Response Centre for the Mediterranean Sea (REMPEC) database, which contains 225 constituents.

Being initially designed for short-term runs (De Dominicis et al., 2013a), the MEDSLIK-II code required customization to cover the entire Mediterranean with 25-day simulations. Consequently, photochemical oxidation and bacterial biodegradation needed to be parameterized. For computational optimization, we employed a simplified first-order oil

[2] https://digitaltwinocean.mercator-ocean.eu (Accessed online: November 2024).

[3] https://www.medslik-ii.org (Accessed online: January 2025).

decay term as follows:

$$\frac{dV^{TK}}{dt} = \left.\frac{dV^{TK}}{dt}\right|_{(E)} - \left.\frac{dV^{TK}}{dt}\right|_{(D)} - \left.\frac{dV^{TK}}{dt}\right|_{(S)} - \lambda V^{TK}$$
$$\frac{dV^{TN}}{dt} = \left.\frac{dV^{TN}}{dt}\right|_{(E)} - \left.\frac{dV^{TN}}{dt}\right|_{(D)} + \left.\frac{dV^{TN}}{dt}\right|_{(S)} - \lambda V^{TN} \quad (1)$$

where V^{TK} and V^{TN} are the oil volumes of the thick and thin parts of the slick. The suffixes indicate evaporation (E), dispersion (D), and spreading (S). The last right-hand terms describe the decay with a constant rate of $\lambda = 0.04\ \text{day}^{-1}$ (Liubartseva et al., 2024). A similar term was used to simplify the total oil weathering over the large spatial scale of the US outer continental shelf (Ji et al., 2021). It was also applied to the relatively small Mediterranean subbasin when the researchers worked with the fine-resolution unstructured computational grid, which required considerable memory capacity (Quattrocchi et al., 2021).

We used a 1 % windage coefficient instead of the JONSWAP-based Stokes drift to reduce the computation time required for the Monte Carlo simulations. Applying this simplification dates back to the classical book of Kinsman (1965) but might introduce some minor biases (<5 % in the Mediterranean), particularly, in the Gulf of Lion and south of Crete. For optimization, we also decreased the number of Lagrangian particles from 100,000 to 40,000 for each virtual spill. The solution appears almost unaffected by this decision, as only a reduction of at least two orders of magnitude could lead to a significant loss of accuracy (De Dominicis et al., 2013b).

Notably, MEDSLIK-II, as a Lagrangian model, preserves sharp gradients of oil concentration. Particle advection can be simulated with high accuracy without any numerical diffusion. In addition, parallelizing the MEDSLIK-II simulations made the problem viable for high-performance computing (HPC).

2.2. Meteo-oceanographic datasets

MEDSLIK-II requires sea currents, sea surface temperatures, and atmospheric wind data to force oil drift and weathering. The Monte Carlo statistics critically depend on the reliability of the datasets representing these significant drivers. In this work, we utilized the Copernicus Marine Service products, which offer free, high-quality information that has proven reliable in actual oil spill cases. We employed daily reanalysis data on currents and temperatures with a horizontal resolution of 1/24° (~4.5 km) and 141 unevenly spaced vertical levels (Escudier et al., 2021). *In-situ* data from CTD ('conductivity, temperature, and depth', ship measurements), ARGO floats (profiling floats), and XBT (expendable bathythermographs) were assimilated into the model in combination with satellite altimetry observations.

We also employed the 10-m wind datasets provided by the European Centre for Medium-Range Weather Forecasts (ECMWF) at a 6-h frequency and a 0.125° horizontal resolution (~12.5 km in the Mediterranean).

3. Oil spill scenario, Monte Carlo simulations, and hazard mapping

3.1. The HAVEN oil spill as a prototype for computation

For the Monte Carlo simulations of accidental oil spills, we focused on the historical *HAVEN* oil spill (off the Port of Genoa, 1991), which is recognized as the largest shipwreck in European waters and one of the worst oil pollution cases in the Mediterranean.

According to the historical records, on 11 April 1991, while the very large crude carrier (VLCC) *HAVEN* was anchored in front of the Port of Genoa, two explosions started a fire on the ship that was extinguished only 70–99 h later when the *HAVEN* sank. At the moment of the disaster, which killed six crew members, 144,000 tons of heavy Iranian crude oil and 1223 tons of fuel oil and diesel were on board. The vessel split into three sections, one sinking close to where the anchor was located. A large quantity of burnt oil rapidly spilt in the form of bitumen. At the same time, currents and waves transported the rest of the cargo in the densely populated coastal region of the Ligurian Sea.

The post-accident environmental assessment indicated substantial injury to subtidal *Posidonia/Cymodocea* (seagrass) beds, the deep-sea benthic community, and associated commercial fisheries (Martinelli et al., 1995). Although the International Tanker Owners Pollution Federation Limited (ITOPF, 2014b) expected recovery within one to three years, a restoration program initiated 12 years later revealed the tar residuals on the seabed and the oil products still contained in the wreck.

The *HAVEN* oil spill is ranked among the five major oil spill incidents documented in the Mediterranean Sea during the 2000s (Table 1).

A simplified *HAVEN* oil spill scenario was used to represent the continuous 50-h release of heavy Iranian crude oil (API[4] = 31) with a 200 ton hour^{-1} spill rate, leading to a total spilled oil volume of 10,000 tons (Martinelli et al., 1995; IOPC Funds, 1991; Daniel et al., 2003; Amato, 2003). The simulation length adopted was 25 days (600 h). We assumed that this duration would be sufficient for the discharged oil to evaporate, disperse, or be beached in the Mediterranean. An initial spin-up period of 25 days was introduced, starting the virtual release of oil from 7 December 2017, to sustain the temporal continuity of the modeled oil concentration fields. The oil spill distributions for this period were subsequently excluded from the statistical analysis.

3.2. Monte Carlo simulations and hazard mapping

The virtual spills were randomly sampled in time from 2018 to 2021. Stratified sampling was conducted throughout the Mediterranean basin, using a manual digitizing algorithm applied to a map published by Dong et al. (2022). The workflow details are available in Fig. S1 in the Supplementary material and Liubartseva et al. (2024). The four-step algorithm imported the normalized area of oil slicks in a 0.1° grid, as shown in Fig. 3B by Dong et al. (2022), into Google Earth. Next, we manually digitized the map using a 1° grid binning. An optimal interpolation procedure was then implemented to re-grid the previous coarse resolution results to a finer resolution of 1/24°, aligning with the corresponding spatial resolution of the Copernicus Marine Service hydrodynamics. Finally, we seeded the proportional number of virtual spills per cell, thereby conducting the stratified Monte Carlo sampling.

Table 1
The *HAVEN* oil spill compared to the five most recent major oil spills in the Mediterranean.

Source	Date	Location	Spill volume	Oil type
HAVEN explosion and wreck	April 1991	Off the Port of Genoa (Ligurian Sea)	~10,000 tons	Crude oil
JIYYEH power plant (Lebanon)	July 2006	Eastern Levantine	~15,000 tons	Heavy fuel oil
Tanker *Agia Zoni II* wreck	September 2017	Saronic Gulf (Aegean Sea)	~2.2 tons	Heavy fuel oil
Ulysse-Virginia collision	October 2018	Off the Cap of Corse (Ligurian Sea)	~520 tons	Heavy fuel oil
Unknown	February 2021	Israeli coastlines	~550 tons	Crude oil
BANIYAS power plant (Syria)	August – September 2021	Eastern Levantine	~12,000 tons	Crude oil

[4] Oil classification by the American Petroleum Institute (API).

An example where 10,000 virtual spill sources are sampled over the Mediterranean is shown in Fig. 1. At least six concentration areas are clearly visible: (1) the Mediterranean adjacent to the Gibraltar Strait, (2) the Algerian coastal zone in the vicinity of the Port of Algiers, (3) the Ligurian Sea maritime sector north of the Strait of Bonifacio, (4) the bunkering areas along the coast of Malta, (5) the Otranto Strait, and (6) the Port Said including the entrance to the Suez Canal. Dong et al. (2022) associated these clusters with ship-induced oil pollution. Other areas are represented by diffuse non-uniform source distributions.

In the results, a sample composed of i virtual spills, $i = 1, \ldots, N$ constitutes the hourly oil concentration fields $C_i^j(x,y)$ at the sea surface and coastlines, where x and y are the longitude and latitude of the bin respectively, $j = 1, \ldots, 600$ is time in hours. Each concentration field is quantized using a simple dimensionless step-function $H\left(C_i^j\right)$ defined for each spill i at the sea surface and coastline:

$$H\left(\max_j C_i^j(x,y)\right) = \begin{cases} 1, \max_j C_i^j(x,y) > THR \\ 0, \max_j C_i^j(x,y) \le THR, \end{cases} \quad (2)$$

where $THR = 0.1$ ton km^{-2} denotes the threshold sea surface concentration and 0.01 ton km^{-1} on the coastline, i.e., the values that, if exceeded, could lead to destructive events (Liubartseva et al., 2021).

The probabilities of oil exceeding the prescribed threshold are represented by the hazard indices $P(x, y)$:

$$P(x,y) = N^{-1} \sum_i^N H(C_i(x,y)). \quad (3)$$

Hazard indices ranged between 0 and 1, where 1 denotes the maximum hazard and 0 indicates no hazard. Considering hazard indices at the sea surface, we used the maximum oil concentrations in Eq. (2). For coastal hazards, the maximum oil concentration can be substituted by the 600-h values as oil accumulates on the coastlines.

The hazard indices were computed on one arc-minute grid (~1.5 km in the Mediterranean), without compromising computational efficiency and visualization accuracy.

4. Results

More than two million simulated virtual spills from 2018 to 2021 enabled us to study the conditional probability of a large accidental oil spill, such as the *HAVEN* catastrophe, occurring in the future at a specific location in the Mediterranean.

4.1. Oil pollution hazard indices

Starting our analysis from the hazard maps for the sea surface and coastline (Fig. 2), the hazard indices values were relatively small, barely reaching 10^{-2}. Such orders of magnitude were expected as the initial sources of the oil spill were highly distributed across the entire domain. These values are consistent with the OSRA-based probability maps for the Gulf of Mexico (Ji et al., 2021), where the initial sources were also highly distributed (though homogeneously) across the basin. In general, unlike highly distributed sources, a point source provides the largest hazard indexes, asymptotically approximating a value of one. Numerous examples of point-source sampling have been reported when assessing hazards or risks from oil production platforms (e.g., French McCay et al., 2017; Olita et al., 2019; Zodiatis et al., 2021).

We observed that the sea surface hazard patterns tended to correspond to the distributions of the oil spill sources (Fig. 1), with some spatial distortions controlled by the meteo-oceanographic conditions in the basin. The concentration and dissipation of oil during accidents can be attributed to the key role played by meteorological conditions. Distinctive 'hot spots,' where the hazard indices values exceed $5.6{\cdot}10^{-3}$, were visible in the Algerian subbasin and the eastern Alboran Sea, the Ligurian Sea, and the center of the Ionian Sea. Intermediate values of hazard indices ranging from $3.5{\cdot}10^{-3} \div 4.5{\cdot}10^{-3}$ were observed in the Balearic Sea, in the northern Tyrrhenian, southern Adriatic, and the entire Levantine.

Conversely, the southern part of the Ionian, the areas east of Sardinia and west of Corsica, the Gulf of Lion, the northern Adriatic, and the north-eastern Aegean Sea did not reveal high hazards.

In addition to the dependence on the sources mentioned above, the spatial distribution of hazard indices was also associated with the combined effect of sea surface currents and 1 % wind speed (Fig. 3). As current velocities tend to dominate over the Stokes drift approximated by 1 % wind speed (Fig. S2, S3 in the supplementary material), the basin-scale circulation features are also visible on the averaged 2018–2021 combined map in Fig. 3. Figs. 2a and 3 show how virtual oil spills concentrated in the Gibraltar area (Fig. 1) have been transferred by the Atlantic Water Current (AWC) and Algerian Current (AC). The coastal Algerian source cluster stretches and restructures in terms of hazards under the Algerian Current (AC), Southern Sardinia Current (SSC), and Eastern Corsica Current (ECC).

The Ligurian cluster is transported mainly by the Eastern Corsica

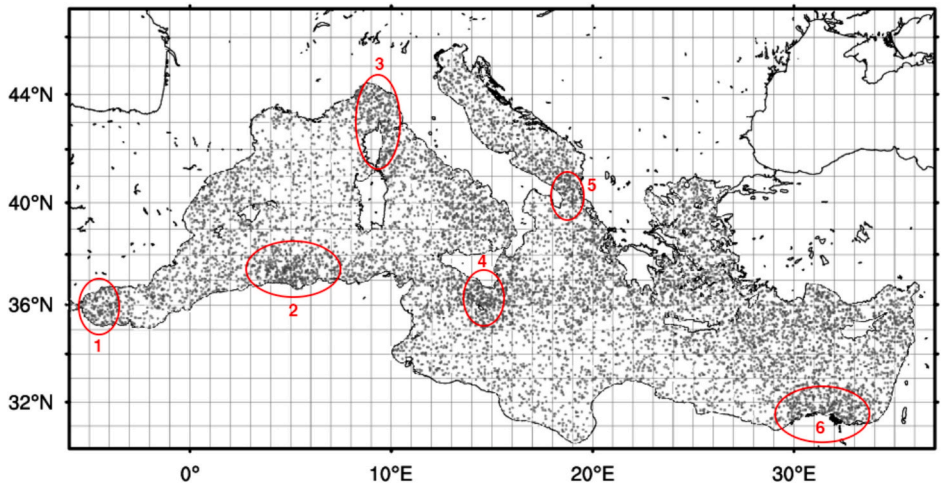

Fig. 1. An example of 10,000 sources of virtual spills sampled according to Dong et al. (2022). Six concentration areas outlined in red are associated with (1) the Gibraltar Strait, (2) the extended Port of Algiers, (3) the north Ligurian Sea sector, (4) the bunkering areas of Malta, (5) the Otranto Strait, and (6) the extended Port Said. (For interpretation of the references to color in this figure legend, the reader is referred to the web version of this article.)

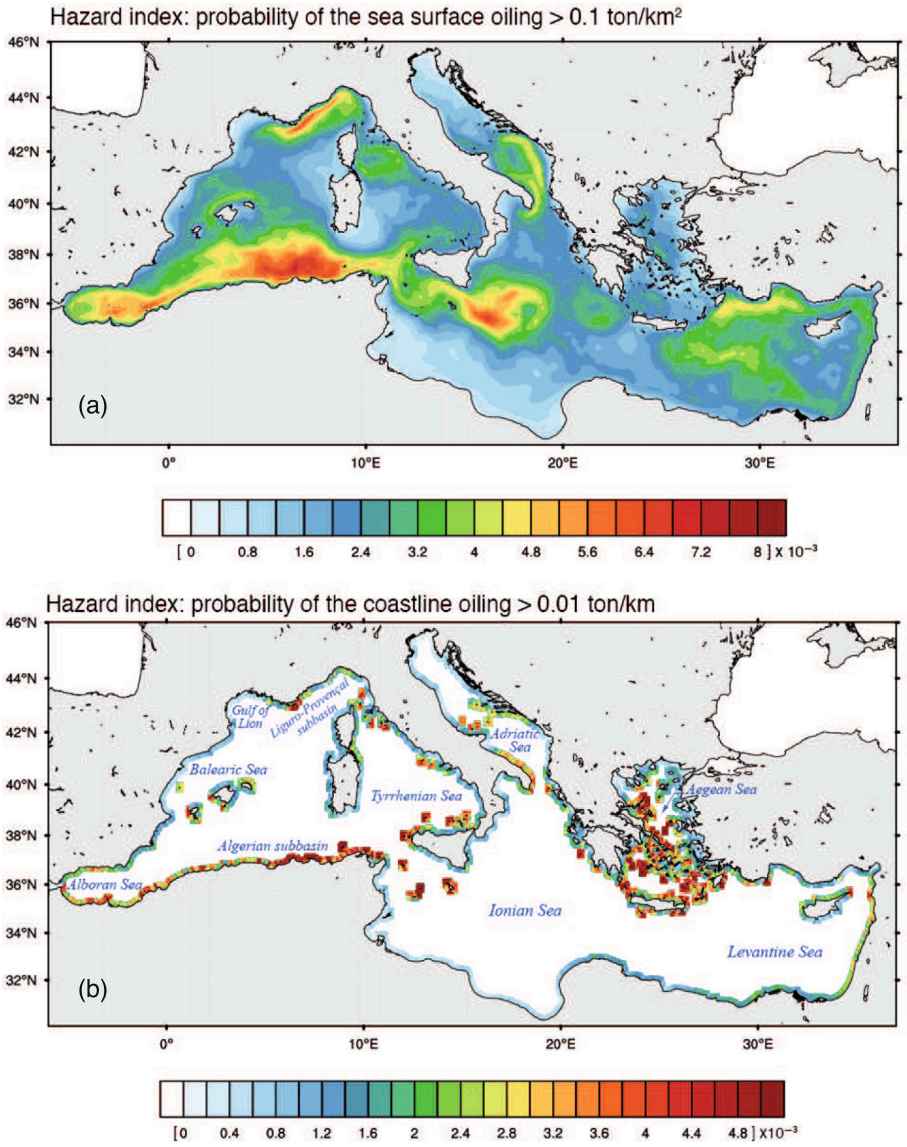

Fig. 2. Hazard indices in probability terms at the sea surface (a) and coastlines (b).

Current (ECC) and Northern Current (NC). The sources associated with the Malta bunkering zone are advected by the Atlantic-Ionian Stream (AIS) and efficiently dissipated in the Central Ionian Sea. The Otranto Strait cluster follows the Western Adriatic Current (WAC) and, is partially trapped by the South Adriatic Gyre (SAG). The spills sampled in the adjacent area of the Suez Canal demonstrate the direct influence of the Cretan Passage Southern Current (CPSC), Asia Minor Current (AMC), and Southern Levantine Current (SLC).

The coastline geometry plays a significant role in the distribution of hazard indices on the coastline. Higher hazard indices are visible on the coastlines of the Alboran Sea and, particularly, the Algerian subbasin and the western tip of Sicily. Moderate hazard levels are found on the Italian southern shores of the Adriatic and the eastern coast of the Levantine Sea. However, maximum coastal hazards are shown in the Aegean Sea, where the ragged shores of archipelagos and numerous small islands result in massive oil beaching. Due to this filtering effect, sea surface hazards in these areas are rather small. Similar partitioning is visible in the archipelagos of the Ionian and Southern Tyrrhenian seas.

For example, zooming in on the Western Mediterranean (Fig. 4a) and the Aegean Sea (Fig. 4b), reveals a detailed hazard distribution along the coastline.

Aside from the southern shores of the Western Mediterranean, which extend from Morocco through Algeria to Tunisia, relatively high hazard levels are observed for the southern Tyrrhenian islands, including the Aeolian Archipelago, Ustica, Aegadian Islands, and the Galite Islands. In contrast, the mid and northern Tyrrhenian islands (Campanian Archipelago, Pontine Islands, and Tuscan Archipelago) exhibit lower hazard levels, with a clear distinction between the windward and leeward sides controlled by the meteo-oceanographic conditions.

In the Aegean Sea, the highest hazard indices are primarily found in the Greek Exclusive Economic Zone (EEZ), which includes the Sporades, Cyclades, the coastlines of Crete, and the Myrtoan Sea. Differences between windward and leeward sides are also evident, making some island shores, such as Antikythera, quite vulnerable, while others, such as the coastlines of the Thracian Sea and Thermaic Gulf, appear more sheltered. The northern coastline of Crete shows significantly higher hazard levels than the southern coastline. The shores of Rhodes indicate moderate to high hazards, particularly along the eastern coast.

The Adriatic coastline, in general, shows relatively small hazard indices apart from the Tremiti Islands and the Salento peninsula (Fig. S4). The Ionian Sea and the central Mediterranean also show high hazards only on the shores of some islands, including the Maltese Archipelago, Pantelleria Island, the Pelagie Islands, Strofades, the Gavdopoula and Gavdos islands (Fig. S5). In the Levantine Sea, the eastern

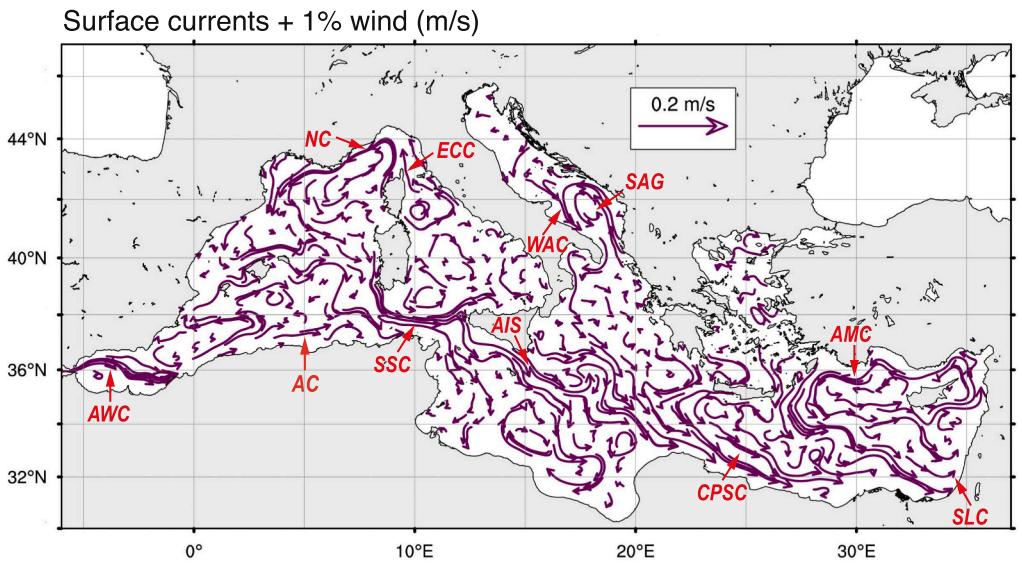

Fig. 3. Averaged 2018–2021 combined forcing (m s^{-1}): sea surface currents +1 % wind with evident basin-scale circulation patterns: the Atlantic Water Current (AWC); Algerian Current (AC); Northern Current (NC); Eastern Corsica Current (ECC); Southern Sardinia Current (SSC); Atlantic-Ionian Stream (AIS); Western Adriatic Current (WAC); South Adriatic Gyre (SAG); Cretan Passage Southern Current (CPSC); Asia Minor Current (AMC); and Southern Levantine Current (SLC).

coastline from Israel to Syria shows higher hazards than the southern segments (Fig. S6). On the Turkish shores, the hazard index peaks at the Cape Gelidonya.

4.2. Arrival time

In this work, we define the arrival time as the interval during which oil first reaches the coastline after the start of the spill. The histogram (Fig. 5a) illustrates the relative frequency of the arrival time in particular class ranges and approximates in discrete form a corresponding probability density function (PDF).

The obtained PDF is bimodal, with a global maximum of approximately 25.6 % for the bin exceeding 25 days. This maximum is not shown in Fig. 5a, as we focused on the information that the histogram was able to provide rather than on the limitations of method, which will be described later. In the given range, the highest frequency of ~5.1 % shows an arrival time of less than one day. We then observe a gradual decrease in occurrence frequency to 1.7 % within a 24–25-day interval.

Compared to the PDF, the cumulative distribution function (CDF) clearly illustrates that the overall probability distribution is bimodal, with approximately 74.4 % of virtual spills reaching the coastline within 25 days (Fig. 5b). We also found a 50 % probability of oil reaching the coast within 13.4 days. Given the positively skewed histogram, we mapped the distribution of the median as a central estimate (Fig. 5c). The map has a horizontal resolution of 1/16° (approximately 6.5 km in the Mediterranean). At least 60 virtual spills were sampled from each grid cell. For consistency, the same color scales were applied to both the histogram and the map. The map shows the circum-Mediterranean continental distribution, with the shortest arrival times forming a coastal strip along the contour of the domain. The Aegean Sea and the eastern part of the Adriatic, which are well-known for their many islands, showed the shortest arrival times, ranging from 1 to 4 days. Intermediate levels of approximately 5–12 days are visible in many areas, including the Alboran Sea, the Strait of Sicily, and the Cilician Sea. With an expected delay of about 13–16 days, the spills would arrive from the Sardinian Channel and the Otranto Strait. If a spill occurred in the Gulf of Lion, southern Adriatic, Cretan Passage, or the areas west of Cyprus, it would take approximately 17–20 days to reach the coast with a 50 % probability. Broad, white-colored areas in the centers of the Western Mediterranean, Tyrrhenian Sea, Ionian Sea, Levantine Sea, and northern Adriatic indicate starting locations from where oil would reach the coast after 25 days. Interestingly, the area north of the Malta bunkering sites (Fig. 1) is flushed by the Atlantic-Ionian Stream so intensively that the corresponding arrival times are quite long. Significant normal-to-shore gradients in the northwestern and southeastern Ionian Sea and northwestern Levantine demonstrate that the nearby shores seem to be naturally sheltered from oil pollution.

CDFs computed for the five predefined Mediterranean subbasins (Fig. 6, Table 2) revealed both similarities and differences in oil spill delivery to the coastlines. We concluded that a simulation duration of 25 days was sufficient for the Aegean Sea, where the average arrival time was roughly 3.1 days, which is the shortest one, and therefore, this subbasin should have the fastest response. In the Adriatic Sea, approximately 87.6 % of the virtual spills would reach the coast with a median arrival time of about 10.7 days (Fig. 7S), followed by the Western Mediterranean. Statistically, the arrival time distribution in this subbasin is the most similar to that of the Mediterranean Sea. The Levantine Sea shows approximately 67.6 % of the beached spills with a median arrival time of about 17.6 days, while in the Ionian Sea and Central Mediterranean, only 57.6 % of spills would reach the beach within 25 days (Fig. 7S). This subbasin also has the highest median arrival time value of approximately 20.6 days (Table 2).

4.3. Oil mass balance

The oil mass balance diagram provides vital information on the temporal redistribution of potentially spilled oil: floating on the sea surface, evaporated, washed ashore, degraded, and dispersed in the water column. Sample mean values and standard deviations of these components are shown in Fig. 7. According to the model simulations, approximately 42.4 % of the oil would presumably evaporate within the first 73 h, which is typical of crude oil (Fig. 7a). After that, evaporation would almost stop. The percentage of evaporated oil, controlled mainly by the oil API, tends to deviate slightly from its average value. The contribution of beaching gradually increases, gaining 11.1 % ± 16.5 % at the end of the simulations. Natural dispersion shows a monotonic rise, reaching 8.4 % ± 4.1 % at the end of the 25-day simulations. Degradation grows exponentially and exceeds the mean dispersion value 56 h after release (Fig. 7b). At the end, the contribution of degradation reaches 29.6 % ± 9.0 %.

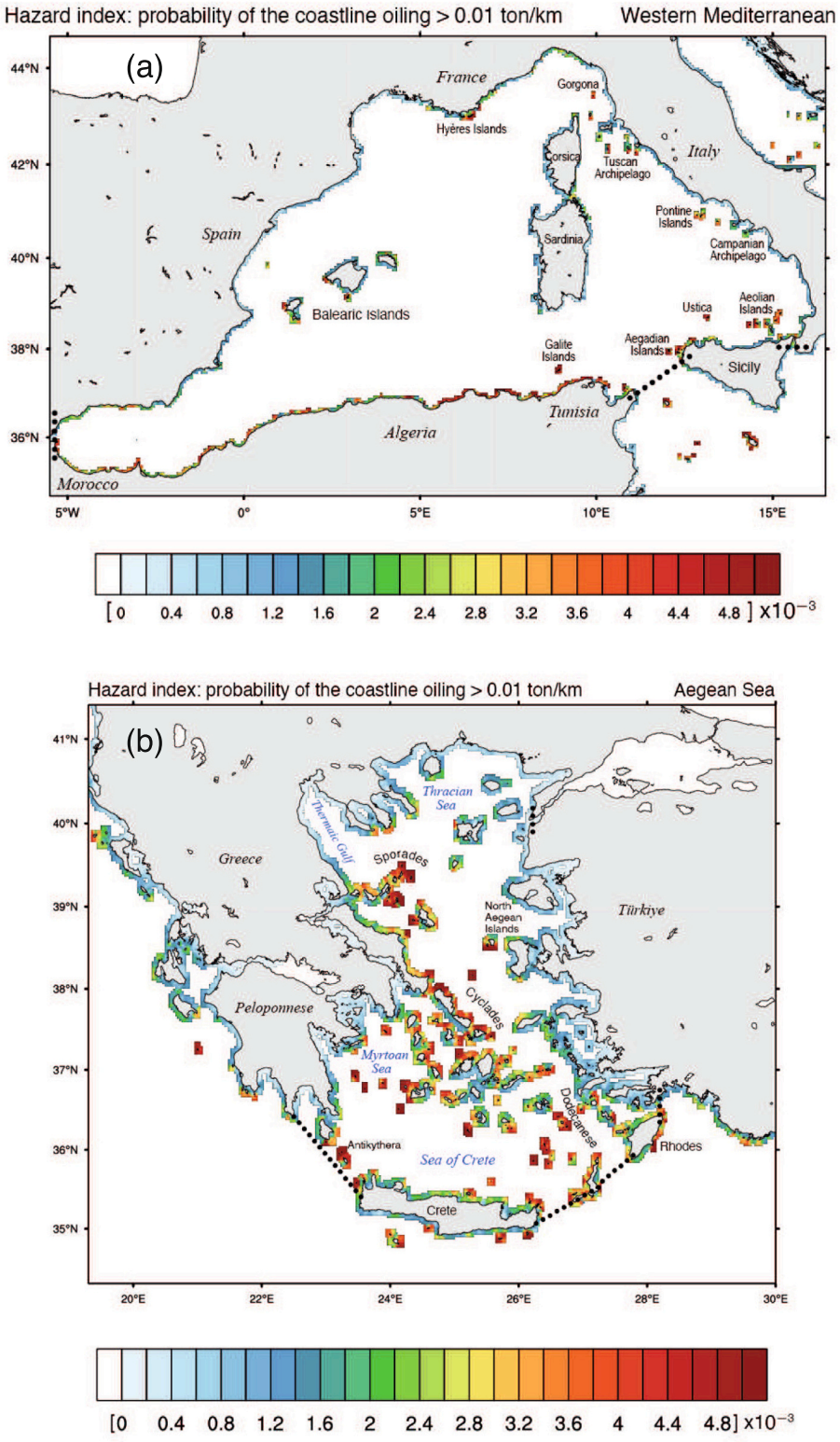

Fig. 4. Zooming in on coastal hazard maps of the Western Mediterranean (a) and Aegean seas (b).

4.4. Percentage of beached oil

When a spill occurs with a known oil volume, it is vital to evaluate in advance the percentage of oil that will eventually be beached on the coastlines (Fig. 8).

We now present the corresponding PDF (Fig. 8a), which is also bimodal as with the arrival time histogram (Fig. 5a). We found that approximately 27.9 % of the sampled virtual spills resulted in the beaching of <2 % of the oil released. The maximum percentage of the beached oil ranged from 56 % to 60 %. The beached oil map was calculated using the median due to the positively skewed histogram (Fig. 8c). Fig. 8a and c are illustrated with the same but inverted color scale as in Fig. 5a and c in order to highlight that the arrival time is inversely related to the beached oil percentage. The longer the arrival

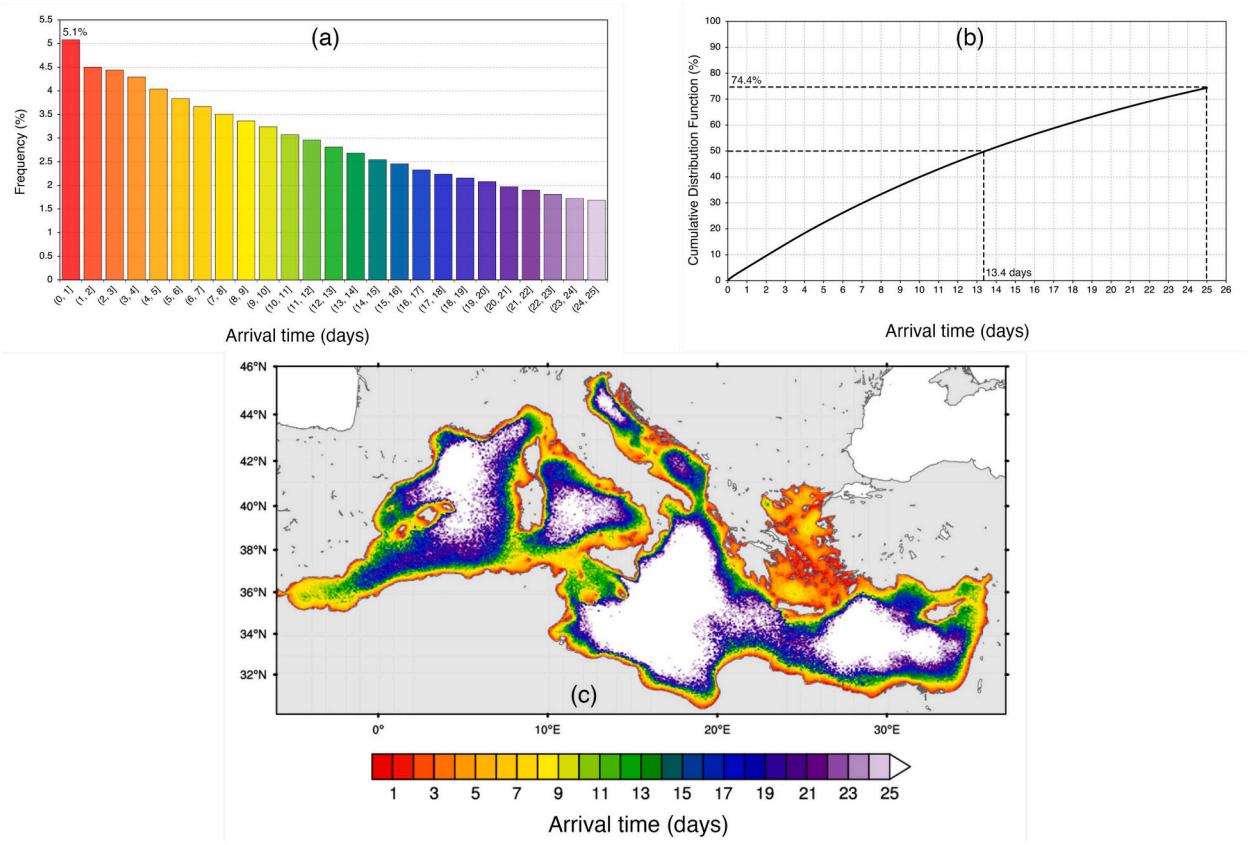

Fig. 5. Histogram of arrival times in days (a), CDF (Cumulative Distribution Function) (b), and the distribution of the median across the basin (c).

time, the lower the rate of the beached oil on the shoreline.

Comparing CDFs for different subbasins, the largest median value of approximately 30.5 % of beached oil occurs in the Aegean Sea, followed by the Adriatic Sea with 4.0 % (Fig. 8b, S). Other subbasins, such as the Western Mediterranean, Levantine Sea, Ionian Sea, and Central Mediterranean, show a sharp decline in the medians from 1.1 % to 0.3 % and 0.2 %, respectively. In Fig. 8c, the map shows that the width of the coastal belt with the high beached oil percentage is rather irregular. Unsurprisingly, the patterns associated with high oil beaching are evident in the Aegean Sea and Adriatic. The belt surrounds almost all of the southern Mediterranean border, becoming thinner along some Algerian and Libyan coastal segments. In contrast, this belt is hardly visible in the Northwestern Mediterranean and the Northwestern Ionian. Interestingly, there are pronounced contrasts between the opposite sides of some big islands: Corsica, Sardinia, Sicily, Crete, Cyprus, and Rhodes.

4.5. *Explicit comparison of basin's and subbasins' statistics*

To underscore the similarities and differences among the Mediterranean subbasins, the hazard indices, arrival times, and beached oil percentages are summarized in Table 3. Because the corresponding histograms were skewed, the medians (M) were selected as a measure of central tendency. The first quartile (Q_1) and third quartile (Q_3) quantify the dispersions of the corresponding model outputs.

Oil spills in the Western Mediterranean, Ionian, Central Mediterranean, and Levantine Sea primarily threaten pelagic ecosystems, from phytoplankton to megafauna (such as sea turtles, mammals, and seabirds). In contrast, the oil that spills in the Aegean and Adriatic seas tends to be beached more quickly and abundantly. This finding should be applied only statistically.

5. Discussion

To test the reliability of the predictions made with the current Monte Carlo simulations, we studied the data[5] collected by the Centre of Documentation, Research and Experimentation on Accidental Water Pollution (CEDRE). Only two cases out of the ten Mediterranean spills found were sufficiently well documented to be compared qualitatively with our results. First, the *Agip Abruzzo* oil spill from the Port of Livorno area (Italy) on 10 April 1991 showed a northward oil drift that qualitatively corresponded to the hazard map in Fig. 2a. The second oil spill from the container ship *Strauss* which occurred off the Port of Genoa-Voltri (Italy) on 19 January 2010, revealed an oil trajectory directed towards the French Côte d'Azur, which also aligned with Fig. 2.

More detailed information can be retrieved from the real cases we simulated for the Regional Marine Pollution Emergency Response Centre for the Mediterranean Region (REMPEC).

In chronological order, first is the *JIYYEH* power plant oil spill (Lebanon, 2006), studied by Coppini et al. (2011). The oil spill moved northeast along the coastline and was beached in good agreement with Fig. 2.

Next, the hazard maps underestimated the *Agia Zoni II* oil spill (Greece, 2017) (Figs. 2a, 4b), although the arrival time was correctly represented (Parinos et al., 2019). This discrepancy likely stems from insufficiently resolved hydrodynamics and orography in the Inner Saronikos Gulf, which we noted during the oil spill emergency response phase (Coppini et al., 2018).

Observational data on the *Ulysse-Virginia* oil spill (North of Corsica, 2018) include overflight records, satellite-derived images, and beach

[5] https://wwz.cedre.fr/en/Resources/Spills (Accessed online: November 2024).

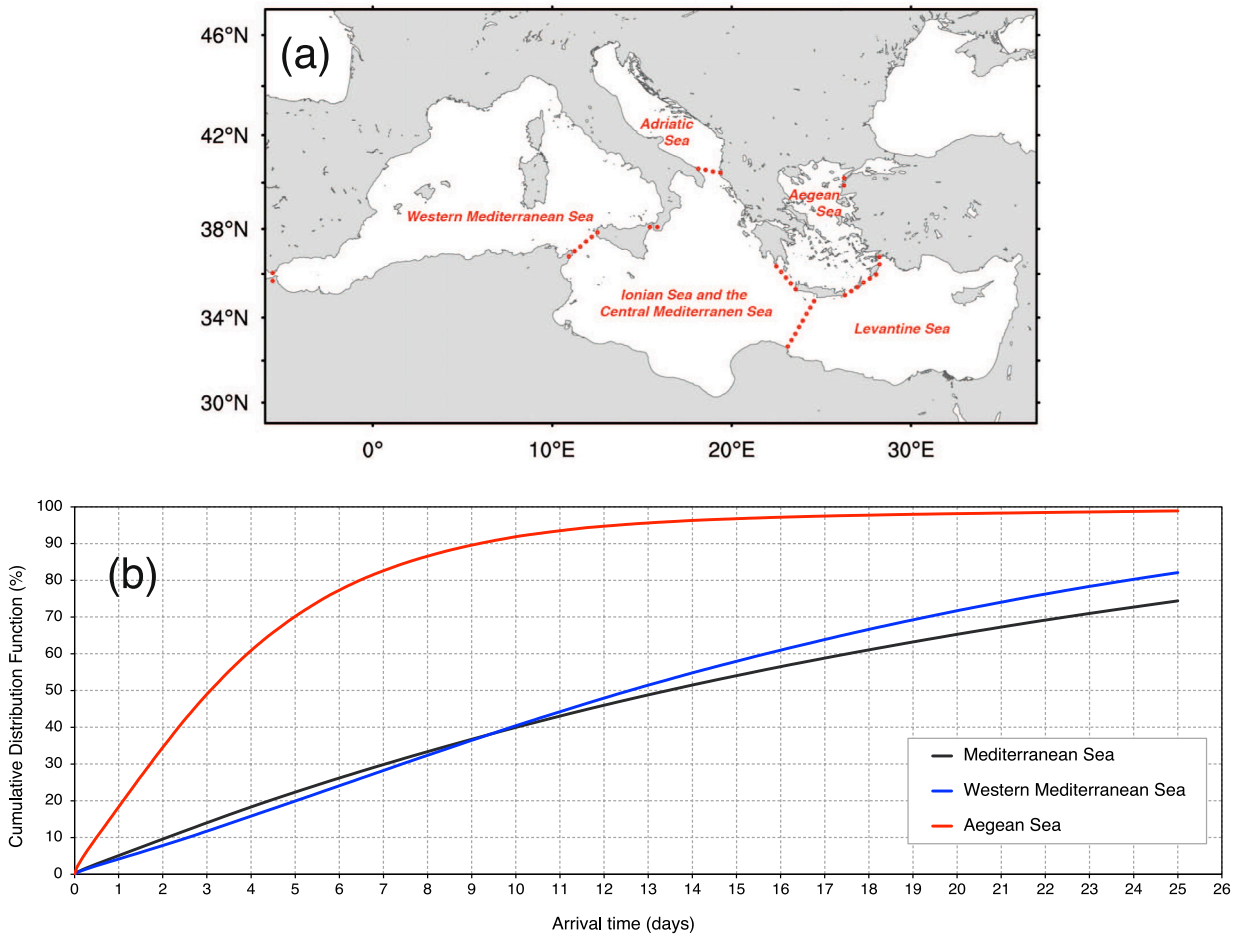

Fig. 6. Pre-defined Mediterranean subbasins (a) and arrival time CDFs (b) for the Mediterranean Sea, Western Mediterranean, and Aegean Sea.

Table 2
Arrival time statistics for the Mediterranean and subbasins.

Basin or subbasin	Percentage of spills reaching the coast within 25 days (600 h)	Median: with a probability of 50 %, oil would reach the coast within:
Mediterranean Sea	74.4 %	~13.4 days (323h)
Western Mediterranean	82.1 %	~12.6 days (302h)
Aegean Sea	98.9 %	~3.1 days (74 h)
Adriatic Sea	87.6 %	~10.7 days (257 h)
Ionian Sea and the Central Mediterranean	57.6 %	~20.6 days (495 h)
Levantine Sea	67.6 %	~17.6 days (422 h)

pollution reports provided in press releases from the Prefecture of Var. Modeled by three independent research groups (by Météo-France with the MOTHY model, CEDRE with OILMAP, and CMCC with MEDSLIK-II), this case represents a best-practice approach for the fusion of observations with modeling (Daniel et al., 2021; Liubartseva et al., 2020). The hazard distributions (Fig. 2a) align with the actual oil drift and the initial beaching on the coastlines of Saint Tropez and the Hyères Islands (Fig. 4a). The estimated arrival time of approximately 9.5 days and the beached oil fraction of around 4.2 % (Fig. 5c, 8c) also show good agreement with the observation data.

The next case is an oil spill in the Mediterranean of unknown origin which caused a massive tar pollution event on the Israeli shoreline in 2021. The hazard distributions (Fig. 2) and arrival time estimations of around 16–17 days match the observational and previous model-derived results (Herut et al., 2024; Liubartseva et al., 2022).

The drift of the oil spilled from the *BANIYAS* power plant (Syria, 2021), as studied in Keramea et al. (2023), corresponds to the hazard maps in Fig. 2. The arrival time and the percentage of beached oil align with the maps in Figs. 5c, 8c, according to the tracking of the satellite-derived slicks (Keramea et al., 2023). However, this comparison does not seem very convincing as the spill originated from the land.

Since Monte Carlo virtual spill sampling has not yet become routine in oil spill modeling, the ground-truth evaluation remains largely qualitative. The quantity and quality of available observations for the spills mentioned above are often incomparable. For example, a hindcast of oil spill pollution from the *JIYYEH* power plant that lasted 28 days was based on several low-resolution satellite-derived images (Coppini et al., 2011). In contrast, while working on the *Agia Zoni II* oil spill, which lasted five days, we had reliable data from both satellites and the local authority overseeing the oil beaching: timing, oil thickness, and patchiness (Coppini et al., 2018).

Before discussing the method's limitations, three main uncertainties typically influencing Lagrangian oil spill modeling need highlighting: uncertainty in the forcing (currents, wind, waves), turbulent diffusivity, and windage coefficient. The uncertainty associated with currents often outweighs the influence of other factors. However, with progress in operational oceanography, which enhances the underlying physics and spatiotemporal resolution, this uncertainty is increasingly less (e.g., Clementi et al., 2017). Diffusivity parameterization has been controversial since the last century (e.g., Okubo, 1971; Murthy, 1977). Considering the recommended values of 1–100 m^2 s^{-1} (ASCE Task Committee on Modeling of oil spills of the Water Resources Engineering Division, 1996), horizontal diffusion is often parameterized through

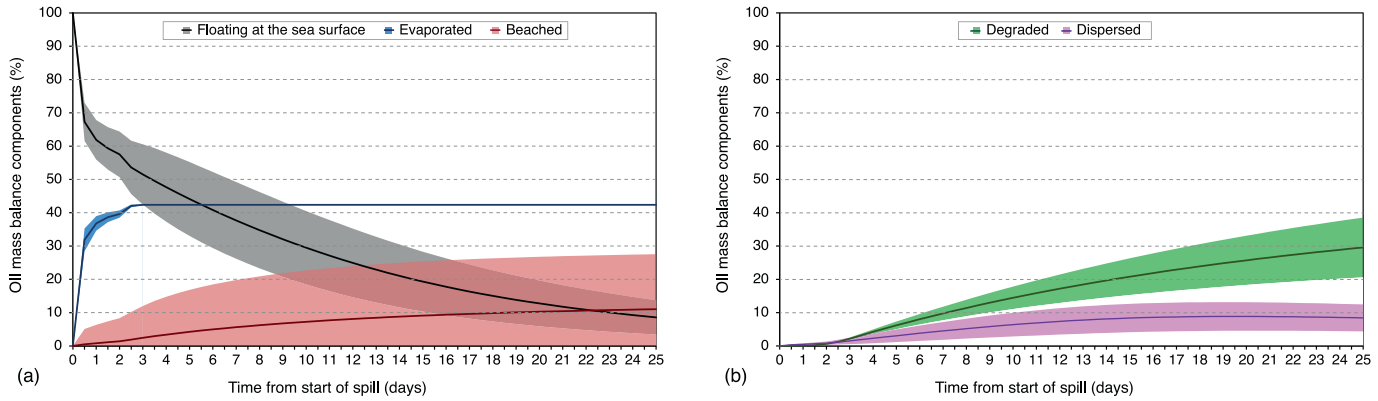

Fig. 7. Oil mass balance diagram showing the distribution of oil (%): at the sea surface, evaporated, beached (a), degraded, and dispersed in the water column (b). Shaded areas depict the spread (mean value ± standard deviation).

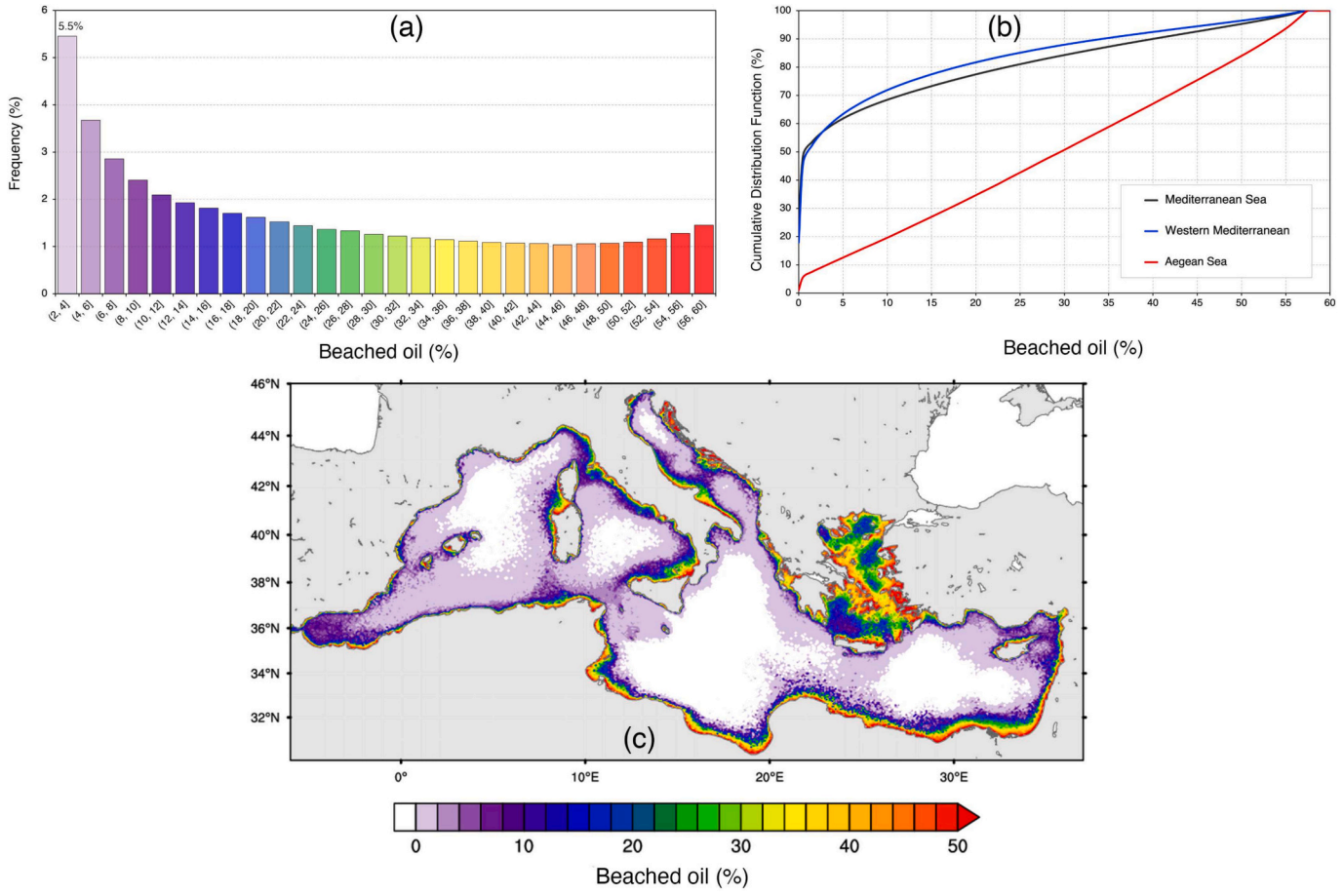

Fig. 8. Histogram of beached oil in % (a), CDFs for the Mediterranean and two selected subbasins (b), the distribution of the median across the basin (c).

Table 3
Basin's and subbasins' statistics summary.

Basin or subbasin	Sea surface hazard $\times 10^{-3}$			Coastline hazard $\times 10^{-3}$			Arrival time (days)			Beached oil (%)		
	Q_1	***M***	Q_3	Q_1	***M***	Q_3	Q_1	***M***	Q_3	Q_1	***M***	Q_3
Mediterranean Sea	2.1	**4.0**	4.3	1.9	**2.6**	3.2	5.7	**13.4**	>25	0.2	**0.5**	16.8
Western Mediterranean	2.7	**4.2**	4.4	1.7	**2.4**	2.6	6.3	**12.6**	21.4	0.3	**1.1**	13.4
Aegean Sea	0.2	**0.7**	0.8	3.6	**4.1**	4.3	1.4	**3.1**	5.6	13.5	**30.5**	44.5
Adriatic Sea	0.9	**1.2**	1.5	0.9	**2.0**	2.2	4.8	**10.7**	18.4	0.4	**4.0**	23.5
Ionian and Central Med	1.1	**3.8**	4.0	0.8	**1.9**	2.0	9.3	**20.6**	>25	0.1	**0.2**	4.0
Levantine Sea	2.6	**3.0**	3.7	1.2	**2.1**	2.3	9.0	**17.6**	>25	0.1	**0.3**	13.5

Q_1 is the first quartile; ***M*** is median or the second quartile; Q_3 is the third quartile.

isotropic scale-dependent constant diffusion coefficients (Matsuzaki and Fujita, 2017). In this work, we used a default value of 2.0 m^2 s^{-1} (De Dominicis et al., 2013a).

The windage coefficient is typically considered to be a tuning parameter that ranges from 0 % to 6 %. However, it does not appear random. Calibration of the windage coefficient for oil, drifters, and other floating objects has been extensively discussed in the literature (e.g., Kim et al., 2014). Finding the optimal windage coefficient may require an iterative approach, which is greatly influenced by the experience and models used by the oil modeling team. For example, the MEDSLIK-II group employs 0 % as a first-guess estimate, whereas the MOTHY team adjusts the coefficient based on wind conditions.

The uncertainties mentioned above influence, to some extent, any oil spill modeling efforts. Practical implications may include inaccuracies in spatiotemporal predictions of the oil spill's trajectory at sea, beaching, or an imbalance in the oil mass. Interested readers should refer to the extensive case-specific literature, which is beyond the scope of this paper.

As the initial source distribution plays a key role in our methodology, manually digitizing the maps published by Dong et al. (2022) limits the adequacy of the Monte Carlo sampling. An underestimation of oil pollution hazards in coastal areas could be one of the practical consequences. Private sector resources, such as the Cerulean[6] system run by SkyTruth (Raphael and Schatz, 2024), need to be involved in scientific research to ensure the availability of robust long-term inventory in digital format.

Additionally, the source map (Dong et al., 2022) has a limitation connected to the radar-derived detection methodology related to an optimal wind speed interval of 1.5–10 m s^{-1}. The bias in this context is not assumed to be significant, as evidenced by the NCEP wind speed statistics in the Mediterranean, where the frequency of lower wind speeds (<1.5 m s^{-1}) is 0.09 ± 0.09 and higher wind speeds (>10 m s^{-1}) is 0.08 ± 0.07 (Dong et al., 2022, Supplementary materials).

The white areas on the maps (Figs. 5c, 8c) indicate that a simulation length of 25 days is insufficient for the entire Mediterranean and the highly dissipative subbasins (the Ionian Sea, Central Mediterranean, Levantine Sea, and Western Mediterranean). The simulation length needs to be extended to address these gaps. According to Spanoudaki (2016), tackling this problem may require a more accurate representation of the biogeochemical degradation term. Lengthening both the simulation duration and degradation complexity could require additional computational resources.

The values of the concentration thresholds in hazard mapping are critical since they control the loss of the oil concentration PDF tails in Eq. (2). Moreover, because there are no strict conventional criteria for selecting them, the resulting uncertainty hinders the comparability of hazard maps computed by different research groups. Currently, three types of thresholds are distinguished: biological, socioeconomic, and those linked to response efficiency. Interested readers can find the dedicated literature review in Liubartseva et al. (2021). The biological thresholds are typically species-specific, and measuring the population response values is challenging. The values we used represent the socioeconomic thresholds linked to mariculture, fishing, ports, water supply intakes, coastal-dependent businesses, tourism, and aesthetics. Importantly, these values were close to the 10 % percentile of the oil concentration PDFs. Such a formal criterion can be applied in the absence of a priori information about the thresholds.

6. Conclusion

Extensive Monte Carlo simulations were carried out to predict the consequences of future oil spills in the Mediterranean Sea. We conducted a virtual spill sampling in the entire Mediterranean from 2018 to 2021 with the MEDSLIK-II model, using the methodology developed by BOEM for the US outer continental shelf. The sampling scenario was derived from the historical *HAVEN* oil spill that took place off the Port of Genoa in 1981. MEDSLIK-II was forced by the Copernicus Marine Service hydrodynamics and ECMWF winds at high resolution.

Distributions of oil pollution hazard indices in probabilistic terms indicate which sea areas and coastlines will be most or least affected when an oil spill occurs in the future. The NECCTON project aims to integrate hazard indices into multiple pressure assessments in the marine environment (Melaku Canu et al., 2024). Statistics on the arrival time and the percentage of oil that reaches the shore reveal a spatiotemporal pattern of oil-fouling shorelines. This information can help improve response strategies and assist in planning for future offshore oil production and high-risk maritime oil transfer activities. Additionally, this work provides the baseline information necessary to conduct more advanced numerical experiments in the academic landscape.

The coastline of the Aegean Sea showed the highest impact, characterized by high coastal hazard indexes, short arrival times, and significant proportions of beached oil. In contrast, the Ionian, Central Mediterranean, and Levantine seas showed low hazard indices, longer arrival times, and smaller percentages of beached oil, which can be attributed to their natural, highly dissipative properties.

A combination of the Monte Carlo technique and the Lagrangian MEDSLIK-II oil spill model could be applied in any area, facilitating further advancements in the representation of natural processes and enhancements in risk assessment. Such simulations are particularly relevant in heavily trafficked marine environments. Possible spills from offshore oil production fields can also be sampled using the Monte Carlo technique. Additionally, risky ship-to-ship oil transfers require environmental assessment for legal regulation, which can be conducted using our methods.

In the future, the enhanced observational oil spill inventory, the upgraded MEDSLIK-II codes, and high-resolution hydrodynamics featuring advanced representations of underlying physics will strengthen the preparedness and resilience against oil spill accidents.

CRediT authorship contribution statement

Svitlana Liubartseva: Writing – review & editing, Writing – original draft, Software, Methodology, Conceptualization. **Giovanni Coppini:** Writing – review & editing, Writing – original draft, Project administration, Conceptualization. **Pierre Daniel:** Writing – review & editing, Writing – original draft, Methodology, Data curation, Conceptualization. **Donata Melaku Canu:** Writing – review & editing, Writing – original draft, Supervision, Methodology, Conceptualization. **Megi Hoxhaj:** Writing – review & editing, Writing – original draft, Software, Data curation.

Declaration of competing interest

The authors declare that they have no known competing financial interests or personal relationships that could have appeared to influence the work reported in this paper.

Acknowledgments

This work was carried out within the framework of the NECCTON project (Horizon Europe RIA under grant number 101081273).

Appendix A. Supplementary data

Supplementary data to this article can be found online at https://doi.org/10.1016/j.marpolbul.2025.118061.

[6] https://cerulean.skytruth.org/?zoom=1.5&lat=29.5&lng=0.2 (Accessed online: December 2024).

Data availability

Data will be made available on request.

References

Amato, E., 2003. An environmental restoration program 12 years after: the *HAVEN* wreck. Les journées d'information CEDRE – 6 oct. 2003. In: Traitement des épaves potentiellement polluantes.

ASCE Task Committee on Modeling of oil spills of the Water Resources Engineering Division, 1996. State-of-the-art review of modeling transport and fate of oil spills. J. Hydraul. Eng. 122, 594–609.

Barron, M.G., Vivian, D.N., Heintz, R.A., Yim, U.H., 2020. Long-term ecological impacts from oil spills: comparison of *Exxon Valdez*, *Hebei Spirit*, and *Deepwater Horizon*. Environ. Sci. Technol. 54, 6456–6467.

Clementi, E., Pistoia, J., Delrosso, D., Mattia, G., Fratianni, C., Storto, A., Ciliberti, S.A., Lemieux-Dudon, B., Fenu, E., Simoncelli, S., Drudi, M., Grandi, A., Padeletti, D., Pietro, P.D., Pinardi, N., 2017. A 1/24 degree resolution Mediterranean analysis and forecast modeling system for the Copernicus Marine Environment Monitoring Service. In: Proceedings of the 8th EuroGOOS International Conference, pp. 275–284.

Coppini, G., De Dominicis, M., Zodiatis, G., Lardner, R., Pinardi, N., Santoleri, R., Colella, S., Bignami, F., Hayes, D.R., Soloviev, D., Georgiou, G., Kallos, G., 2011. Hindcast of oil spill pollution during the Lebanon Crisis, July–August 2006. Mar. Pollut. Bull. 62, 140–153.

Coppini, G., Gonzalez, G., Perivoliotis, L., Smaoui, M., Liubartseva, S., Bourma, E., Lecci, R., Cretì, S., 2018. MONGOOS-REMPEC operational experience during *Agia Zoni II* oil spill, September 2017. In: Geophys. Res. Abs, (EGU2018–6745–1).

Daniel, P., Marty, F., Josse, P., 2003. Impact of the progress in operational oceanography on oil spill drift forecasting in the Mediterranean Sea. Elsevier Oceanogr. Ser. 69, 218–221.

Daniel, P., Paradis, D., Gouriou, V., Le Roux, A., Garreau, P., Le Roux, J.F., Louazel, S., 2021. Forecast of Oil Slick Drift from *Ulysse*/CSL *Virginia* and *Grande America* Accidents. Int. Oil Spill Conf. Proc., p. 1141410

De Dominicis, M., Pinardi, N., Zodiatis, G., Lardner, R., 2013a. MEDSLIK-II, a Lagrangian marine surface oil spill model for short term forecasting–part 1: theory. Geosci. Model Dev. 6, 1851–1869.

De Dominicis, M., Pinardi, N., Zodiatis, G., Archetti, R., 2013b. MEDSLIK-II, a Lagrangian marine surface oil spill model for short-term forecasting – part 2: numerical simulations and validations. Geosci. Model Dev. 6, 1871–1888.

Dong, Y., Liu, Y., Hu, C., MacDonald, I.R., Lu, Y., 2022. Chronic oiling in global oceans. Science 376, 1300–1304.

Escudier, R., Clementi, E., Cipollone, A., Pistoia, J., Drudi, M., Grandi, A., Lyubartsev, V., Lecci, R., Aydogdu, A., Delrosso, D., Omar, M., Masina, S., Coppini, G., Pinardi, N., 2021. A high resolution reanalysis for the Mediterranean Sea. Front. Earth Sci. 9, 1060.

French McCay, D.P., 2009. State-of-the-Art and Research Needs for Oil Spill Impact Assessment Modeling. Proceedings of the AMOP Technical Seminar, pp. 601–653.

French McCay, D.P., Balouskus, R., Ducharme, J., Schroeder Gearon, M., Kim, Y., Zamorski, S., Li, Z., Rowe, J., Perham, C., Wilson, R., 2017. Potential Oil Trajectories and Surface Oil Exposure from Hypothetical Discharges in the Chukchi and Beaufort Seas. Proceedings of the AMOP Technical Seminar, pp. 660–693.

Goldman, R., Biton, E., Brokovich, E., Kark, S., Levin, N., 2015. Oil spill contamination probability in the Southeastern Levantine basin. Mar. Pollut. Bull. 91, 347–356.

Herut, B., Goldman, R., Ozer, T., Lazar, A., Biton, E., Gertman, I., Silverman, J., Segal, Y., Sisma-Ventura, G., Gertner, Y., Rubin-Blum, M., Belkin, N., Rahav, E., 2024. Tar pollution event (2021) at the Southeastern Levantine oligotrophic basin, short-term impacts and operational oceanography perspectives. Mar. Pollut. Bull. 198, 115892.

IOPC Funds, 1991. Annual Report 1991. Repro Workshop Ltd, Alton, Hampshire, Great Britain. https://iopcfunds.org/wp-content/uploads/2018/12/1991_ENGLISH_ANNUAL_REPORT.pdf.

ITOPF, 2014a. Effects of Oil Pollution on Fisheries and Mariculture. Technical Information paper #11.. Impact PR & Design Limited, Canterbury, UK https://www.itopf.org/fileadmin/uploads/itopf/data/Documents/TIPS_TAPS_new/TIP_11_Effects_of_Oil_Pollution_on_Fisheries_and_Mariculture.pdf.

ITOPF, 2014b. Effects of Oil Pollution on the Marine Environment. Technical Information paper #13.. Impact PR & Design Limited, Canterbury, UK https://www.itopf.org/fileadmin/uploads/itopf/data/Documents/TIPS_TAPS_new/TIP_13_Effects_of_Oil_Pollution_on_the_Marine_Environment.pdf.

Ji, Z.G., Li, Z., Johnson, W., Auad, G., 2021. Progress of the oil spill risk analysis (OSRA) model and its applications. J. Mar. Sci. Eng. 9, 195.

Keramea, P., Kokkos, N., Zodiatis, G., Sylaios, G., Coppini, G., Peña, J., Benjumeda, P., Sepp Neves, A.A., Lardner, R., Liubartseva, S., Soloviev, D., Scuro, M., Nikolaidis, A., Viola, F., 2023. Satellite imagery in evaluating oil spill modelling scenarios for the Syrian oil spill crisis, summer 2021. Front. Mar. Sci. 10, 1264261.

Kim, T.H., Yang, C.S., Oh, J.H., Ouchi, K., 2014. Analysis of the contribution of wind drift factor to oil slick movement under strong tidal condition: *Hebei Spirit* oil spill case. PloS One 9, e87393.

Kinsman, B., 1965. Wind Waves: Their Generation and Propagation on the Ocean Surface. Prentice-Hall, Englewood Cliffs, N.J, p. 676.

Landrigan, P.J., Stegeman, J.J., Fleming, L.E., Allemand, D., Anderson, D.M., Backer, L. C., Brucker-Davis, F., Chevalier, N., Corra, L., Czerucka, D., Bottein, M.D., Demeneix, B., Depledge, M., Deheyn, D.D., Dorman, C.J., Fénichel, P., Fisher, S., Gaill, F., Galgani, F., Gaze, W.H., Giuliano, L., Grandjean, P., Hahn, M.E., Hamdoun, A., Hess, P., Judson, B., Laborde, A., McGlade, J., Mu, J., Mustapha, A., Neira, M., Noble, R.T., Pedrotti, M.L., Reddy, C., Rocklöv, J., Scharler, U.M., Shanmugam, H., Taghian, G., van de Water, J., Vezzulli, L., Weihe, P., Zeka, A., Raps, H., Rampal, P., 2020. Human health and ocean pollution. Ann. Glob. Health 86, 151.

Li, Z., Smith, C., DuFore, C., Zaleski, S.F., Auad, G., Johnson, W., Ji, Z.G., O'Reilly, S.E., 2021. A multifaceted approach to advance oil spill modeling and physical oceanographic research at the United States Bureau of Ocean Energy Management. J. Mar. Sci. Eng. 9, 542.

Liubartseva, S., Smaoui, M., Coppini, G., Gonzalez, G., Lecci, R., Cretì, S., Federico, I., 2020. Model-based reconstruction of the *Ulysse-Virginia* oil spill, October–November 2018. Mar. Pollut. Bull. 154, 111002.

Liubartseva, S., Federico, I., Coppini, G., Lecci, R., 2021. Stochastic oil spill modeling for environmental protection at the Port of Taranto (Southern Italy). Mar. Pollut. Bull. 171, 112744.

Liubartseva, S., Zodiatis, G., Coppini, G., Sepp Neves, A.A., Peña, J., Benjumeda, P., Lecci, R., Soloviev, D., 2022. Operational simulations of a Mediterranean oil spill in February 2021. In: Geophys. Res. Abs, (EGU2022–2276).

Liubartseva, S., Coppini, G., Daniel, P., Hoxhaj, M., 2024. Modeling the high-impact low probability oil spills in the Mediterranean. In: Proceedings of the 10th International Symposium: Monitoring Mediterranean Coastal Areas, Livorno, Italy, 11–13 June, 2024, pp. 911–922.

Martinelli, M., Luise, A., Tromellini, E., Saue, T.C., Neff, J.M., Douglas, G.S., 1995. Proceedings of International Oil Spill Conference, Long Beach, California, US, 27 February–2 March 1995, 1, pp. 679–685.

Matsuzaki, Y., Fujita, I., 2017. In situ estimates of horizontal turbulent diffusivity at the sea surface for oil transport simulation. Mar. Pollut. Bull. 117, 34–40.

Melaku Canu, D., Solidoro, C., Bandelj, V., Quattrocchi, G., Sorgente, R., Olita, A., Fazioli, L., Cucco, A., 2015. Assessment of oil slick hazard and risk at vulnerable coastal sites. Mar. Pollut. Bull. 94, 84–95.

Melaku Canu, D., Leiknes, Ø., Unnuk, A., Rumes, B., Zeppilli, D., Sarrazin, J., Canesi, L., Schumckel, U., Fianchini, M., Korme, I., 2024. A Common Handbook: Cumulative Effects Assessment in the Marine Environment. JPI Oceans, Brussels. https://doi.org/10.48470/77.

Murthy, C.R., 1977. Turbulent diffusion processes in the Great Lakes. Session of UNESCO Sponsored International Higher Hydrological Course (9th, 1977, Moscow, Russia). https://publications.gc.ca/site/eng/9.903325/publication.html.

Okubo, A., 1971. Oceanic diffusion diagrams. Deep-Sea Res. 18, 789–802.

Olita, A., Cucco, A., Simeone, S., Ribotti, A., Fazioli, L., Sorgente, B., Sorgente, R., 2012. Oil spill hazard and risk assessment for the shorelines of a Mediterranean coastal archipelago. Ocean Coast. Manage. 57, 44–52.

Olita, A., Fazioli, L., Tedesco, C., Simeone, S., Cucco, A., Quattrocchi, G., Ribotti, A., Perilli, A., Pessini, F., Sorgente, R., 2019. Marine and coastal hazard assessment for three coastal oil rigs. Front. Mar. Sci. 6, 274.

Parinos, C., Hatzianestis, I., Chourdaki, S., Plakidi, E., Gogou, A., 2019. Imprint and short-term fate of the Agia Zoni II tanker oil spill on the marine ecosystem of Saronikos Gulf. Sci. Total Environ. 693, 133568.

Pizzigalli, C., Rupolo, V., Lombardi, E., Blanke, B., 2007. Seasonal variability dispersion maps in the Mediterranean Sea obtained from the Mediterranean Forecasting System Eulerian velocity fields. Prog. Oceanogr. 22 (C05012), 1–17.

Polinov, S., Bookman, R., Levin, N., 2021. Spatial and temporal assessment of oil spills in the Mediterranean Sea. Mar. Pollut. Bull. 167, 112338.

Price, J., Jonson, W., Marshall, C., Ji, Z.G., Rainey, G., 2003. Overview of the oil spill risk analysis (OSRA) model for environmental impact assessment. Spill Sci. Technol. Bull. 8, 529–533.

Quattrocchi, G., Simeone, S., Pes, A., Sorgente, R., Ribotti, A., Cucco, A., 2021. An operational numerical system for oil stranding risk assessment in a high-density vessel traffic area. Front. Mar. Sci. 8, 585396.

Raphael, J., Schatz, J., 2024. SkyTruth's Cerulean: public database of near-real-time oil detections. In: Geophys. Res. Abs, (EGU2024–13480).

Sharma, K., Shah, G., Singhal, K., Soni, V., 2024. Comprehensive insights into the impact of oil pollution on the environment. Reg. Stud. Mar. Sci. 74, 103516.

Smith, R.A., Slack, J.R., Wyant, T., Lanfear, K.J., 1982. The oil spill risk analysis model of the U.S. In: Geological Survey; Geological Survey Professional Paper 1227; United States Government Printing Office: Washington, DC, USA, p. 40.

Souza, N.G.S., Lugon Jr., J., Yamasaki, E.N., Kyriakides, I., Silva Neto, A.J., 2023. An assessment of relative potential impacts to Cyprus' shoreline due to oil spills in the eastern Mediterranean Sea. J. Integr. Coast. Zone Manag. 23, 27–40.

Spanoudaki, K., 2016. Mathematical modelling of oil spill fate and transport in the marine environment incorporating biodegradation kinetics of oil droplets. In: Geophys. Res. Abs, (EGU2016–13155).

Zodiatis, G., Lardner, R., Liubartseva, S., Sylaios, G., Palazov, A., Kubryakov, A., Ciliberti, S.A., Soloviev, D., Keramea, P., Zhuk, E., Radhakrishnan, H., Yaitskaya, N., Korotaev, G., Coppini, G., Matishov, G., Ioshpa, A., Neprokin, O., Spanoudaki, K., Hadjistassou, C., Kampanis, N., Lisovskyi, R., 2021. Numerical models for oil spillages in the Black Sea and the adjacent sea of Azov. In: The Handbook of Environmental Chemistry. Springer, Berlin, Heidelberg. In book: Angela Carpenter and Andrey G. Kostianoy (eds.), Oil Pollution in the Black Sea: Part I - Monitoring and prevention strategies in the international context. Publisher: Springer, Berlin, Heidelberg, pp. 1–34. https://doi.org/10.1007/698_2021_815.